

FORSTERITIC DETERMINATION OF OLIVINE

BY

XRD ANALYSIS

FORSTERITIC DETERMINATION OF OLIVINE

BY

XRD ANALYSIS

By

Kevin J. D. Ridley

A Thesis

Submitted to the Department of Geology
in Partial Fulfilment of the Requirements
for the Degree
Bachelor of Science

GEOLOGY 4K6

McMaster University

May 1973

TABLE OF CONTENTS

	PAGE
ACKNOWLEDGEMENTS	ii
ABSTRACT	iii
LIST OF TABLES AND FIGURES	iv
INTRODUCTION	1
EXPERIMENTAL PROCEDURE	2
RESULTS AND ERROR DISCUSSION ON EXPERIMENTAL PROCEDURE	20
DISCUSSION	33
CONCLUDING REMARKS AND RECOMMENDATIONS	38
REFERENCES	41

ACKNOWLEDGEMENTS

The author wishes to extend his appreciation to thesis advisors, Drs. R.H. McNutt and H. D. Grundy, for their generous assistance and support given in preparation of this paper. I would also like to thank them for the opportunities provided for this research. The ultra-basic rocks and the olivine of known Fo. composition were provided by Dr. McNutt. The helpful guidance of Dr. D.M. Shaw on the Frantz magnetic separator is also acknowledged.

The assistance of Mr. L.J. Falkiner in XRD preparations and techniques is also greatly acknowledged.

Many thanks are extended to colleagues W.P. Binney, F.C. Hawthorne, P.D. Rice and A.G. Sherin, for many helpful hints, discussions and criticisms.

ABSTRACT

Fo. determinative curves for lattice planes (301), (311), and (401) were calculated from four natural olivines. 2θ values for each olivine were computed from the lattice parameters using the reciprocal lattice d^* for the orthorhombic crystal system

$$d_{hkl}^* = \left[\frac{h^2}{a^2} + \frac{k^2}{b^2} + \frac{l^2}{c^2} \right]^{1/2}$$

combined with the Bragg equation

$$\lambda_{CuK\alpha} = \frac{2 \sin \theta_{hk}}{d_{hkl}^*}$$

XRD patterns for 10 natural olivines were used to determine their respective Fo. composition. Errors were calculated for the Fo. composition of the natural olivines yielding an accuracy from the determinative curves of ± 6 wt. % Fo. An olivine of 90 wt. % Fo. was X-rayed and plotted along the determinative curves giving values of Fo. composition for (301), (311) and (401) of 89, 87 and 85 wt. % respectively.

The effect of Ni, Mn and Ca substituting into the (Mg, Fe) olivine structure causing $\Delta 2\theta$ shifts was also considered and found to be negligible for natural (Mg, Fe) olivines.

LIST OF TABLES AND FIGURES

	PAGE
TABLE I Modal Analysis	3
TABLE II Peak Intensities and Ratios	6
TABLE III Fo. Composition and Lattice Parameters for Fo. Curves	8
TABLE IV Calculated d Spacing and 2θ from Table III	8
TABLE V Conversion Constants.	15
TABLE VI 2θ for Sudbury Samples	19
TABLE VII Fo. Composition and Calculated Fo. Error (Δ Fo.)	21
TABLE VIII Error in Fo. Determinative Curves calculated from Standard Deviation in Lattice Parameters	27
TABLE IX Mean Peak to Background Intensity Ratios and calculated Δ Fo. Composition (wt. % Fo.)	28
TABLE X Olivines of Varying Mg, Fe, Ni, Ca, and Mn Compositions	35
TABLE XI Synthetic Forsterite and Fayalite	36
FIGURE I Fo. Determinative Curves	11
FIGURE II XRD Sample 10, Run 2	18
FIGURE III Mean Peak to Background intensity ratios vs. Δ Fo. 301	29
FIGURE IV " " " " " Δ Fo. 311	30
FIGURE V " " " " " Δ Fo. 401	31

INTRODUCTION

A quick method was developed for determining Fo. composition by XRD analysis. A Fo. determinative curve was constructed from 4 olivines of varying Fo. composition obtained from Birle et al. (1968).

The XRD method applies in this study parallels that of Yoder and Sahama (1957). A plot of 2θ of the (301), (311) and (401) planes versus Fo. composition was used to determine the Fo. composition of 10 olivines from the ultra-basic inclusions in the Sub-layer of Murray Mine, Sudbury.

The purpose of this paper was to test the validity of the Fo. determinative curves using powder XRD data from the 10 Sudbury samples and an olivine of known Fo. composition.

EXPERIMENTAL PROCEDURE

(A) Separation of Olivine from the Whole Rock

The procedure developed in this study can be used for olivine-rich rocks in general. The Sudbury samples were used to establish this method.

The rock samples were crushed, ground in a mortar and pestle, wet sieved between 100 and 200 mesh size, washed in acetone and allowed to dry.

Olivine was separated from the whole rock samples by the Frantz magnetic separator. A hand magnet was used to remove any strongly magnetic minerals such as pyrrhotite and magnetite prior to placement in the Frantz. This precaution was taken as up to 15% of the modal composition of some of these rocks consists of these strongly magnetic minerals. The modal analysis was done by Dr. R.H. McNutt and is displayed in Table I. If these minerals are not removed before placing the sample in the magnetic separator, they have a tendency to form aggregates and cause inhomogeneous separation.

Best separation of olivines in the magnetic separator occurs when calibrated at 25° forward tilt and 15° side tilt (personal communica-

TABLE I MODAL ANALYSIS

SAMPLE	2	4	5	6	7	8	9	10	11	12
Plag.	10.88	3.16	4.25	2.40	1.18	9.39	4.98	4.40	7.60	3.40
F.G. Plag.	14.69	-	-	-	-	15.26	-	-	-	-
Opx.	5.73	7.69	24.25	26.60	8.06	26.03	25.40	25.40	16.40	13.40
Cpx.	-	-	1.50	1.00	0.20	0.20	0.32	1.60	0.40	0.20
Olivine	64.69	55.23	39.00	15.20	44.60	12.72	12.86	48.40	26.20	17.80
Serp.	1.53	26.63	15.50	44.40	29.67	24.85	41.00	12.00	31.20	59.40
Talc.	-	-	-	0.20	-	7.83	0.32	1.00	-	-
Biotite	0.95	0.20	3.50	0.60	3.54	0.20	4.82	1.40	3.40	2.20
Opaques	0.95	6.51	10.50	9.80	11.39	3.52	9.97	6.00	14.60	4.40
Quartz	0.19	0.39	1.25	-	0.60	-	0.16	-	0.20	-

Modal Analysis done by Dr. R.H. McNutt

tion with Dr. D. M. Shaw 1972). Olivines have a magnetic range from 0.3 to 0.5 amperes. Each sample was run starting at 0.5 amperes and ending at 0.2 amperes. After optimum purity was obtained at a particular current setting the current was decreased by 0.1 amperes. Optimum purity was fulfilled by running the sample through the separator at a constant current setting until a complete magnetic separation of the minerals present occurs. This was checked by visual observation while the sample was in the separator. The non-magnetic portion of the sample was saved in a small vial and the magnetic fraction was used for the next run. A completely separated sample consisted of 4 specimens that are non-magnetic at 0.5, 0.4, 0.3 and 0.2 amperes and one magnetic at 0.2 amperes.

Pyroxene is magnetic over a range of 0.4 to 0.7 amperes (personal communication with Dr. Shaw, 1972). This overlaps the olivine field considerably and is very noticeable in the magnetic separation as the modal analysis shows there is a high percentage of pyroxene in most of the samples studied (refer to Table I). This problem is minimized by choosing a specimen from a lower magnetic potential. Choice of a specimen from the lower current amperage was determined through XRD analysis of all 5 fractions from samples No. 4 and No. 5. The intensity of the diffraction peaks was measured for each fraction at each particular current used on the magnetic separator.

The specimen that is non-magnetic at 0.2 amperes yet magnetic at 0.3 amperes has been determined to have the most intense olivine XRD peaks and, therefore, must contain the highest percentage of olivine. Table II illustrates these results. The other 8 samples (No. 2 and Nos. 6-12) were assumed to contain optimum olivine content at the same magnetic potential as No. 4 and No. 5 because all 10 samples were prepared and separated in a similar fashion under the same experimental conditions and the original rock types are of the same ultrabasic nature.

The fraction of the sample that is magnetic at 0.2 amperes should not have any olivine present as this is below the magnetic range of olivines. From observation of Table II, strong residual olivine peaks appear. This was observed when the ratio of magnetic at 0.2 amperes to non-magnetic at 0.2 amperes was calculated. This phenomena occurs because of the fine grained nature of these rocks. Even at the minimal size of 200 mesh, magnetite was preferentially fused to the olivine grains giving some olivine grains a false and greater magnetic potential. As a result, residual peaks were found at such a low magnetic potential.

TABLE II PEAK INTENSITIES AND RATIOS

Peak Intensity in cm.	SAMPLE NO. 4			SAMPLE NO. 5		
	301	311	401	301	311	401
non-magnetic 0.5 amps.	2.6	3.5	0.8	0.9	1.6	0.8
" 0.4 "	1.9	4.5	1.0	1.6	1.9	1.0
" 0.3 "	5.2	5.5	1.4	2.0	2.2	1.2
" 0.2 "	5.6	7.0	2.3	2.2	2.7	1.3
magnetic 0.2* "	3.8	4.3	1.4	1.6	1.8	1.0
peak ratios 0.5/0.2	0.47	0.50	0.35	0.41	0.59	0.62
0.4/0.2	0.34	0.65	0.44	0.73	0.70	0.77
0.3/0.2	0.93	0.79	0.61	0.91	0.82	0.93
0.2/0.2	1.00	1.00	1.00	1.00	1.00	1.00
0.2*/0.2	0.68	0.62	0.61	0.73	0.67	0.77

(B) Preparation of Samples for XRD Analysis

Selection of useful lattice parameters for the construction of a working curve were obtained from Birle et al. (1968). These 4 particular olivines were chosen because they had a wide variation in Fo. composition permitting the construction of a curve to be undertaken with reliable accuracy. The d spacing and 2θ were determined from these parameters. Table III lists the Fo. composition (wt. %) and the lattice parameters.

Before calculating the d spacing and 2θ , selection of suitable lattice planes had to be made. The following factors were considered and resulted in the planes (301), (311) and (401) being chosen.

(1) Sufficient and significant $\Delta 2\theta$ shift between the daltonide compositions of Mg_2SiO_4 and Fe_2SiO_4

$\Delta 2\theta_{301}$	$\Delta 2\theta_{311}$	$\Delta 2\theta_{401}$
0.715°	0.748°	0.996°

(2) Significant intensity

I ₃₀₁ / I	I ₃₁₁ / I	I ₄₀₁ / I
60%	70%	20%

(3) No overlap or interference with any other peaks due to another mineral phase being present.

TABLE III Fo. COMPOSITION AND CORRESPONDING LATTICE PARAMETERS

Fo. Composition (Weight %)	LATTICE PARAMETERS (\AA°)		
	a	b	c
1) Mg _{.90} Fe _{.10}	10.225	5.994	4.762
2) Mg _{.54} Fe _{.46}	10.325	6.038	4.785
3) Mg _{.49} Fe _{.49} Mn _{.01} Ca _{.01}	10.341	6.044	4.787
4) Mg _{.04} Fe _{.92} M _{.04}	10.469	6.099	4.816

DATA from Birle et al. (1968)

TABLE IV CALCULATED d SPACING AND 2θ FROM TABLE III

	d SPACING (\AA°)			2θ (degrees)		
	301	311	401	301	311	401
1	2.7716	2.5157	2.2523	32.299	35.689	40.031
2	2.7940	2.5357	2.2718	32.032	35.398	39.672
3	2.7973	2.5386	2.2747	31.994	35.357	39.619
4	2.8258	2.5640	2.2996	31.662	34.995	39.173

These factors must be fulfilled for ease and precision in measurement or one tends to approximate where a correct measurement should be made.

Olivines are orthorhombic where the symmetry requires $\alpha = \beta = \gamma = 90^\circ$ and the length of the lattice parameters are $a \neq b \neq c$ such that $a > b > c$ (Deer et al.). For the orthorhombic crystal system the reciprocal d spacing

$$d^* = \frac{1}{(d_{hkl})^{2/2}} = \left[\frac{h^2}{a^2} + \frac{k^2}{b^2} + \frac{l^2}{c^2} \right]^{1/2} \quad (1)$$

where a, b and c are the lattice parameters and h, k and l are the corresponding Miller indices. The d spacings can then be determined by taking the reciprocal of d_{hkl}^* (i. e.) $d_{hkl} = \frac{1}{d_{hkl}^*}$

The d spacings are absolute values while 2θ varies with the type of radiation used. $\text{CuK}\alpha$ radiation ($\lambda = 1.5418\text{\AA}$) was used in this study. 2θ was calculated from the Bragg equation

$$\lambda_{\text{CuK}\alpha} = \frac{2 \sin \theta}{d_{hkl}^*} \quad (2)$$

where $2 \sin \theta = (\lambda_{\text{CuK}\alpha}) (d_{\text{hkl}}^*)$ (3)

The data so obtained are tabulated in Table IV.

Three diagnostic curves of 2θ versus Fo. composition for (301), (311), and (401) were constructed. 2θ rather than d was plotted versus Fo. composition for convenience. A 2θ value can be read straight from the XR chart. If d spacings were used, an extra calculation to convert 2θ to d would have to be made. The 3 curves are illustrated in Figure I.

(C) Selection of an Internal Standard

A suitable internal standard was selected. Silicon was chosen for this study since it fulfills the following requirements:

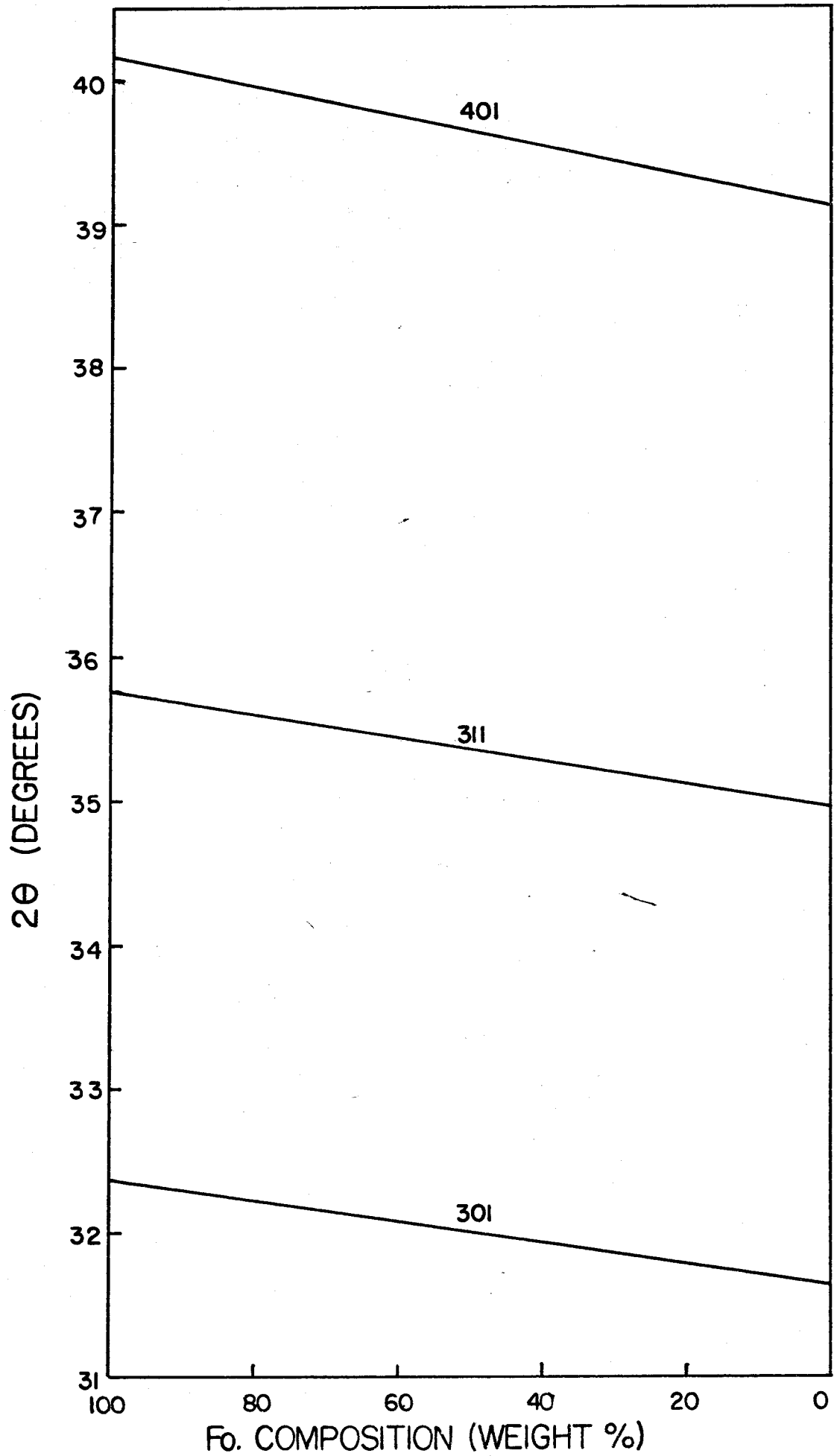
- (1) between a scan range of 25° to 50° silicon has only 2 diffraction trace peaks, (111) at $2\theta = 28.422^\circ$ and (220) at $2\theta = 47.345^\circ$.
- (2) These 2 diffraction trace peaks flank the 3 olivine trace peaks (301), (311) and (401).
- (3) The intensity of each diffraction peak is

$$I_{111}/I = 100\% \text{ and } I_{220}/I = 60\%.$$

- (4) The location of (111) and (220) diffraction trace peaks are distinct and unaffected by the olivine samples and existing impurities.

Quartz, KCl and NaCl were all tried as internal standards but each one of these compounds interfered with one of the diagnostic olivine peaks used in this study.

FIGURE 1 2θ vs F_0 COMPOSITION



(D) Mounting of the Sample

Each specimen was powdered in an agate mortar with acetone. The acetone was drained off and the specimen was left to dry. A hand magnet was passed over the mortar to remove any magnetite which may have been fused to the olivine grains prior to powdering. This precaution reduces the amount of impurity of the sample and background reading in the X-ray traces.

The silicon was powdered in a separate agate mortar with acetone. If silicon and olivine are powdered together they do not mix homogeneously as silicon has a tendency to act as a lubricant for the olivine (personal communication with Dr. H. D. Grundy, 1973). The acetone was drained off and the silicon was left to dry. Silicon was added to the olivine in a ratio of about 1 part standard to 4 parts olivine in an agate mortar with acetone. If this ratio was increased the silicon diffraction peaks became too intense and plotted off the XR chart. The 2 components are mixed until homogeneous and the acetone was drained off.

A small amount of the olivine-silicon mixture was mounted on a glass slide in a slurry using a few drops of nail varnish. The sample is ready for XR analysis.

(E) XRD Analysis

Each sample was placed in a Philips vertical scanning x-ray diffractometer. The current was fixed at 15mA and the voltage in the circuit was 30kV (Dr. H.D. Grundy). A scan range of $2\theta=25^\circ$ to $2\theta=50^\circ$ was used in order to include both silicon and all 3 olivine peaks. Rate of geiger and chart traverse was $1^\circ 2\theta/\text{minute}$ and $1/2''/1^\circ 2\theta$ respectively. The slit size was 1° .

In order for a quantitative analysis of the diffraction peaks to be done the instrument must be set up for optimum resolution. Emphasis on peak separation and intensity must result. These qualities were obtained by scanning each sample at a scale factor of 4, a multiplicity of 1 and a time constant of 8. When the scale factor was increased, the peaks became smaller and less defined. As the scale factor was reduced, the most intense peaks, silicon (111) and olivine (311), ran off the XR chart. The time constant was decreased and more counts per unit time were recorded causing a less smooth curve and hindering accurate measurements. Best results were obtained for each sample at 4/1/8.

The output from the geiger counter was displayed on a calibrated chart. In this study, Copper $K\alpha$ radiation filtered through a graphite crystal monochromator was used to produce the x-ray beam.

Each sample was run a total of 6 times. In order to account for fluctuations in the current causing excitation of the x-ray tube, each specimen was run once until all 10 samples had been run. This precaution was taken to minimize experimental error such that all the samples in one cycle are equally prone to machine fluctuation.

(F) Measurement of 2θ from XR Chart

Measurement of the traces was done on a vernier instrument. This routine consists of measuring a distance in centimetres between the various peaks concerned, converting this distance to degrees and obtaining a 2θ value for each of the 3 olivine peaks. The distance between the silicon standard peaks remained very constant throughout the XR study and corresponds to a $\Delta 2\theta$ (i. e. $2\theta_{220} - 2\theta_{111}$) of 18.923° . This constant, when divided by the mean distance \bar{X} , between the silicon standard peaks for each of the 10 samples yields $\Delta 2\theta'$, a conversion constant unique to each olivine sample where one cm. of distance equals a constant value of $2\theta'$ in degrees. These constants are displayed in Table V.

The distance of all 3 olivine trace peaks per sample were measured relative to the silicon (111) peak and the mean distance $\Delta \bar{X}_{hk\lambda}$ for each peak was calculated. Conversion from cms. to degrees was done by multiplying each mean by $\Delta 2\theta'$ yielding $2\theta'$ values. The $2\theta'$ value corresponds to the difference between the $2\theta_{111}$ of silicon peak and the $2\theta_{hk\lambda}$ of the respective olivine peak. Addition of $2\theta'$ and $2\theta_{111}$ resolves a true $2\theta_{hk\lambda}$ for the olivine peaks.

TABLE V CONVERSION CONSTANTS CALCULATED FOR EACH
SUDBURY OLIVINE

<u>SUDBURY SAMPLE</u>	<u>One CM. = $\Delta 2\theta'$(degrees)</u>
2	0.790
4	0.788
5	0.790
6	0.789
7	0.789
8	0.790
9	0.789
10	0.788
11	0.788
12	0.789

A calculation of 2θ in sample No. 10 follows:

Distance between silicon (111) and (220) was:

	$\Delta X_{\text{silicon}}$
Run No. 1	24.038 cm.
2	24.022 cm.
3	23.952 cm.
4	23.984 cm.
5	24.048 cm.
6	24.064 cm.

$$\bar{X} \quad 24.018 \text{ cm.}$$

$$\begin{aligned} \text{In all cases } \Delta 2\theta_{\text{silicon}} &= (2\theta_{220} - 2\theta_{111}) \\ &= 18.923^\circ \end{aligned}$$

$$\Delta 2\theta' = \frac{18.923^\circ}{24.018 \text{ cm.}} = 0.788^\circ/\text{cm.}$$

Distances of olivine peaks (301), (311) and (401) from silicon (111)

	ΔX_{301} cm.	ΔX_{311} cm.	ΔX_{401} cm.
Run No. 1	4.840	9.152	14.680
2	4.864	9.184	14.616
3	4.794	9.152	14.608
4	4.828	9.152	14.614
5	4.834	9.178	14.632
6	4.890	9.244	14.646
\bar{X}_{hkl}	4.842	9.177	14.633

$2\theta'$ values were calculated via $(\Delta 2\theta') \times (\bar{X}_{hkl})$:

$2\theta'_{301}$	$2\theta'_{311}$	$2\theta'_{401}$
3.816°	7.232°	11.531°

The actual 2θ values of all 3 olivine peaks follows:

$$2\theta_{hkl} = 2\theta_{hkl}' + 2\theta_{(111)}$$

$2\theta_{301}$	$2\theta_{311}$	$2\theta_{401}$
32.238°	35.654°	39.953°

A diffraction trace chart of run No. 2 for sample No. 10 is displayed in Figure II. All of the other 9 samples were calculated in an identical fashion. These results are tabulated in Table VI.

FIGURE II XRD SAMPLE 10, RUN 2

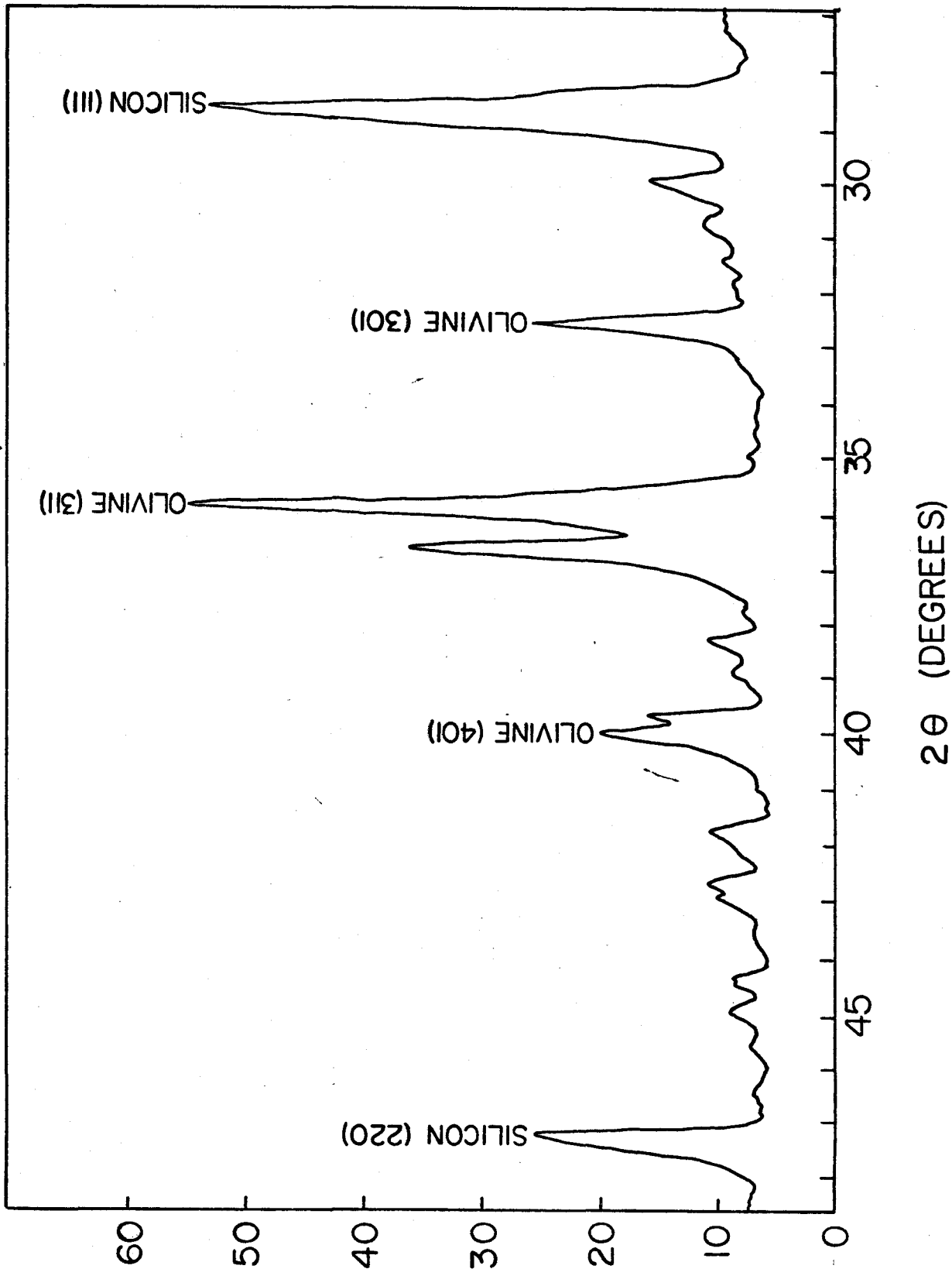


TABLE VI 2θ CALCULATED FROM MEASURED DISTANCE EACH
OLIVINE PEAK WAS FROM SILICON (111)

SUDBURY SAMPLE	$2\theta_{301}$ (degrees)	$2\theta_{311}$ (degrees)	$2\theta_{401}$ (degrees)
2	32.118	*35.504	†39.804
4	32.255	35.676	39.951
5	32.196	35.600	39.893
6	32.217	35.656	39.975
7	32.224	35.622	39.980
8	32.240	35.635	*39.929
9	32.212	†35.630	39.945
10	32.238	35.654	39.953
11	32.245	35.633	39.928
12	32.213	†35.662	39.934

* measurement of 5 of 6 peaks

† measurement of 4 of 6 peaks

RESULTS AND ERROR DISCUSSION ON EXPERIMENTAL PROCEDURE

Once $2\theta_{hkl}$ has been secured, the Fo. composition in weight % can be read directly from one of the curves displayed in Figure I. The Fo. composition for the 10 Sudbury olivine samples are tabulated in Table VII.

Both operator and machine error affect the precision of the results in this study. Handling errors during crushing, sieving and washing plus experimental limitations due to poor separation of olivine from other minerals in the whole rock, all contribute to sample contamination. Further contamination by pyroxene (due to similar magnetic potential) and magnetite (due to fusion of magnetite onto olivine grains because of the fine grained nature of the rock) caused minor shifts in the diffraction peaks. A non-homogeneous smear of the sample on the glass slide constitutes a loss of precision. Observational errors occurred when determining $2\theta_{hkl}$ of the diffraction peaks with respect to:

- (1) eccentricity of the peaks from the idealized symmetrical form,
- (2) location of the centre of the peak on each measurement,
- (3) consistence in measuring exactly to the same position each time, and
- (4) consistent standard to olivine ratio for each sample x-rayed.

TABLE VII Fo. COMPOSITION (Wt. % Fo.) AS READ FROM Fo.
 DETERMINATIVE CURVES AND CALCULATED
 ERROR (Δ Fo.)

SUDBURY SAMPLE	301	311	401
2	66±15	67±5	67±5
4	84±5	87±5	82±4
5	76±5	78±6	76±5
6	79±4	85±4	84±2
7	80±8	81±6	85±6
8	82±4	83±4	80±8
9	78±3	82±3	81±4
10	81±5	85±6	82±4
11	82±12	82±10	79±9
12	78±5	86±8	80±6

Other sources of error result from:

- a) variations in x-ray power supply (Adler, p. 146, 1966)
- b) setting of tube voltage and current "
- c) positioning of x-ray spectrometer "
- d) adsorption of x-rays by the specimen (Azaroff et al., page 211, 1958)

Errors were calculated taking the difference between the mean distance \bar{X}_{hkl} , and the maximum deviation σ_{hkl} , for each peak in every sample. The result, $\Delta\sigma_{max}$ in cms., was first converted to 2θ using the conversion factor $\Delta 2\theta'$ unique to that sample. Next, ΔF_o was determined using the equation of the line corresponding to that lattice plane.

A calculation for sample No. 10 follows. Some of the data listed below was extracted from previous calculations involving sample No. 10.

	(301) cm.	(311) cm.	(401) cm.
\bar{X}_{hkl}	4.842	9.177	14.633
$\sigma_{max. hkl}$	4.890	9.244	14.680
$\Delta\sigma_{max. hkl}$	± 0.048	± 0.067	± 0.047

Conversion of $\Delta\sigma_{max. hkl}$ to 2θ was achieved as follows:

$$(\Delta\sigma_{max. hkl}) \times (\Delta 2\theta')$$

where $\Delta 2\theta'$ for No. 10 = $0.788^\circ/\text{cm}$.

Results were:

$\Delta 2\theta_{301}$	$\Delta 2\theta_{311}$	$\Delta 2\theta_{401}$
$\pm 0.038^\circ$	$\pm 0.053^\circ$	$\pm 0.037^\circ$

The equation of the line $y = mx + b$ for each of the 3 Fo. composition curves in Figure I was used to convert $\Delta 2\theta_{hkl}$ to $\Delta Fo.$ where

$$y_{hkl} = 2\theta_{hkl}$$

m = slope of the line (negative in all cases)

x = Fo. composition

b = y intercept

The slopes and y intercepts were calculated from each curve and are listed below:

	301	311	401
m	-0.0076	-0.0083	-0.0102
b	31.619°	34.950°	39.118°

In order to account for the error in Fo. composition $\Delta 2\theta_{hkl}$ was added to y_{hkl} . The resulting equation for conversion of error calculation from degrees to Fo. composition was

$$(y \pm \Delta 2\theta_{hkl}) = m x' + b$$

where $x' = b - \frac{(y \pm \Delta 2\theta_{hkl})}{m}$

and x' is the maximum error of the Fo. composition.

The detailed calculations follow:

$$x'_{301} = \frac{31.619^{\circ} (32.238 \pm 0.038)}{-0.0076} = 86.447 \text{ wt. \% Fo.}$$

$$x'_{311} = \frac{34.950 - (35.654 \pm 0.053)}{-0.0083} = 91.205 \text{ wt. \% Fo.}$$

$$x'_{401} = \frac{39.118 - (39.953 \pm 0.037)}{-0.0102} = 85.490 \text{ wt. \% Fo.}$$

To arrive at a final error in the Fo. composition

$$\Delta x' = x' - x$$

$$\Delta x'_{301} = 86.447 - 81.447 = \pm 5.000 \text{ wt. \% Fo.} = \pm 5 \text{ wt. \% Fo.}$$

$$\Delta x'_{311} = 91.205 - 84.819 = \pm 6.386 \text{ wt. \% Fo.} = \pm 6 \text{ wt. \% Fo.}$$

$$\Delta x'_{401} = 85.490 - 81.863 = \pm 3.627 \text{ wt. \% Fo.} = \pm 4 \text{ wt. \% Fo.}$$

The other 9 samples were calculated in an identical manner and the results are listed in Table VII.

Another source of error lies in the construction of the 3 determinative curves. These errors originate in the lattice parameters obtained from Birle et al. A standard deviation of $\pm 0.010 \text{ \AA}^\circ$ for parameter a, $\pm 0.006 \text{ \AA}^\circ$ for parameter b and $\pm 0.005 \text{ \AA}^\circ$ for parameter c was listed from the above paper for each of the 4 olivines used to produce the Fo. determinative curves.

To calculate the effect of the standard deviation of each lattice parameter on curve synthesis and resulting accuracy, each standard deviation was added to its respective lattice parameter yielding maximum a, b and c values. Conversion of these maximum parameters to maximum $2\theta_{hkl}$ values follows via equations 1, 2 and 3. Next, the original calculated $2\theta_{hkl}$ values for the olivines involved in the curve synthesis were subtracted from the maximum $2\theta_{hkl}$ submitting a standard deviation for each olivine in degrees. Standard deviation of the 2θ values are listed in Table VIII.

These values were converted to $\Delta\text{Fo.}$ compositions analogous to earlier error calculations using the equation of the line for each curve. Table VIII contains the error in Fo. composition in Wt. %. All 4 olivines for each of the 3 planes with the exception of lattice plane (301) of olivine No. 1 show a variation in wt. % Fo. of ± 4 . As a result, each curve due to uncertainty in exactness of the lattice parameters contains an error of ± 4 wt. % Fo. regardless of the purity of the olivine being determined.

A third error calculation was done. This calculation provides the basis for the overall experimental error in F_o composition determination. Peak to background intensity ratios were computed. The background intensity occurs by diffraction of x-rays having a wavelength other than $K\alpha$, by air scattering (Azaroff et al. 1958) and by impurities present in the sample.

A large peak to background ratio permits more precision in measurement of peaks on the vernier instrument. The greater the precision in measurement the more reliability was emphasized on a peak. Thus a peak that was considered to be very reliable showed a credible error for the experimental procedure.

Peak to background intensity ratios were calculated for each olivine peak on every run for all 10 Sudbury samples. A mean value of peak to background intensity ratio was computed for each olivine peak for every sample. These are tabulated in Table IX along with calculated ΔF_o composition.

Peak to background intensity ratios were graphed versus the calculated error in F_o composition (ΔF_o) for each of lattice planes (301), (311) and (401). Figures III, IV and V illustrate this relationship.

TABLE VIII ERROR IN F_o . DETERMINATIVE CURVES CALCULATED FROM STANDARD DEVIATION IN LATTICE PARAMETERS

	Max. $2\theta_{hkl}$ (deg.)	Calculated $2\theta_{hkl}$ (deg.)	S. D. $\Delta 2\theta_{hkl}$ (deg.)	ΔF_o . (wt. %)
--	--------------------------------	--------------------------------------	--	------------------------

301

1	32.299	32.265	0.034	± 5
2	32.032	32.000	0.032	± 4
3	31.994	31.961	0.033	± 4
4	31.662	31.630	0.032	± 4

311

1	35.689	35.652	0.037	± 4
2	35.398	35.362	0.036	± 4
3	35.357	35.320	0.037	± 4
4	34.995	34.959	0.036	± 4

401

1	40.031	39.989	0.042	± 4
2	39.672	39.632	0.040	± 4
3	39.619	39.578	0.041	± 4
4	39.173	39.133	0.040	± 4

TABLE IX MEAN PEAK TO BACKGROUND INTENSITY RATIOS AND
CALCULATED ΔF_o . COMPOSITION (Wt. %Fo.)

Mean Peak to Background Intensity Ratios			
Sudbury Sample	\bar{X}_{301}	\bar{X}_{311}	\bar{X}_{401}
2	1.07	1.50	1.01
4	5.17	6.90	3.29
5	3.93	7.02	3.32
6	1.23	3.75	2.27
7	3.59	3.51	6.91
8	4.80	7.77	1.89
9	5.20	2.95	1.99
10	3.27	10.78	6.16
11	2.27	3.67	2.33
12	1.93	5.56	2.29

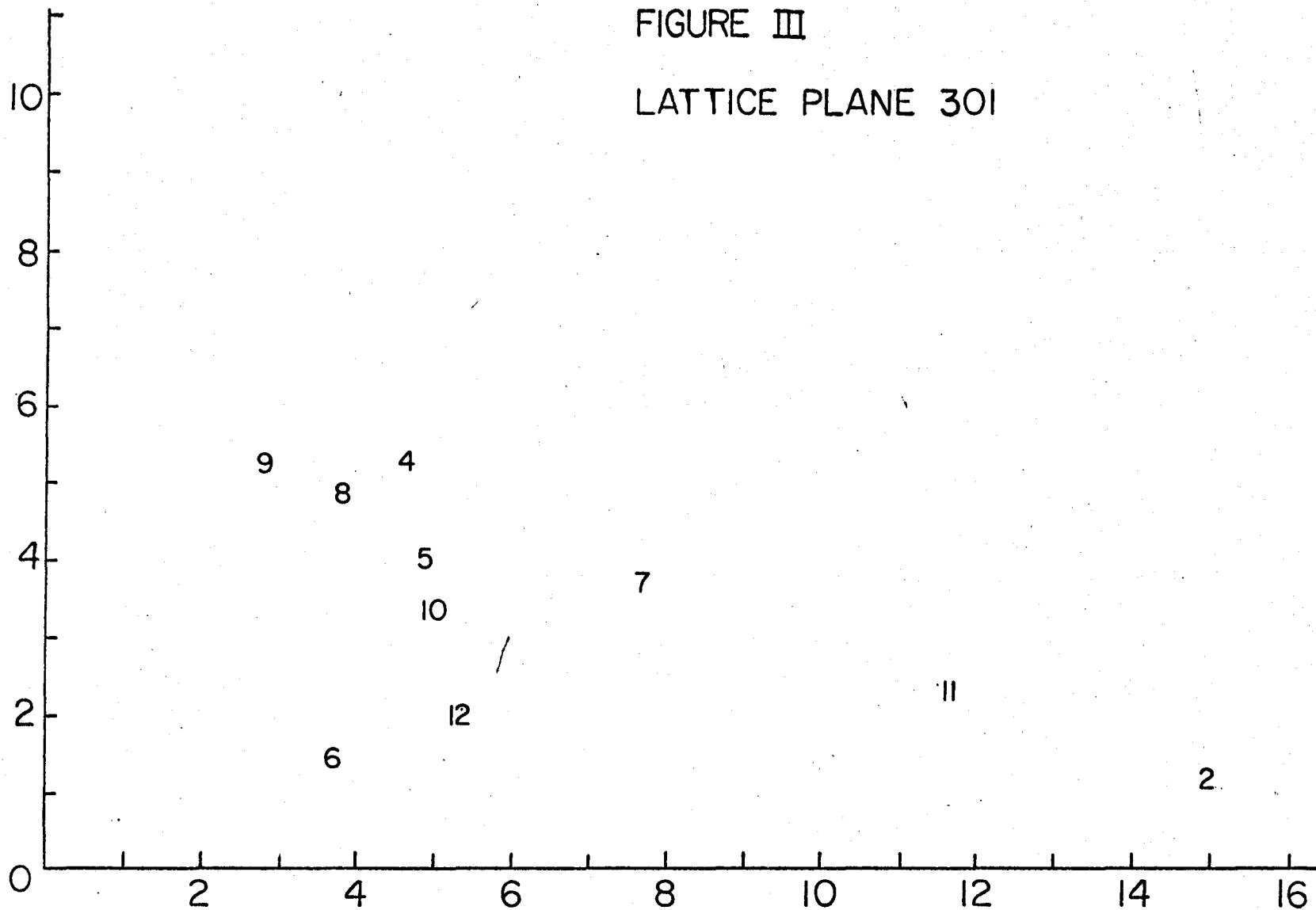
Calculated ΔF_o . Composition (wt. % Fo.)

Sudbury Sample	301	311	401
2	± 15.131	± 4.819	± 4.902
4	± 4.605	± 5.060	± 4.117
5	± 4.868	± 6.145	± 4.510
6	± 3.553	± 3.976	± 2.058
7	± 7.632	± 5.663	± 5.980
8	± 3.684	± 3.615	± 8.333
9	± 2.895	± 3.373	± 3.628
10	± 5.000	± 6.386	± 3.627
11	± 11.711	± 10.121	± 8.921
12	± 5.263	± 7.831	± 6.373

MEAN PEAK TO BACKGROUND INTENSITY RATIOS

FIGURE III

LATTICE PLANE 301



CALCULATED ERROR IN F_o . COMPOSITION (WEIGHT %)

MEAN PEAK TO BACKGROUND INTENSITY RATIOS

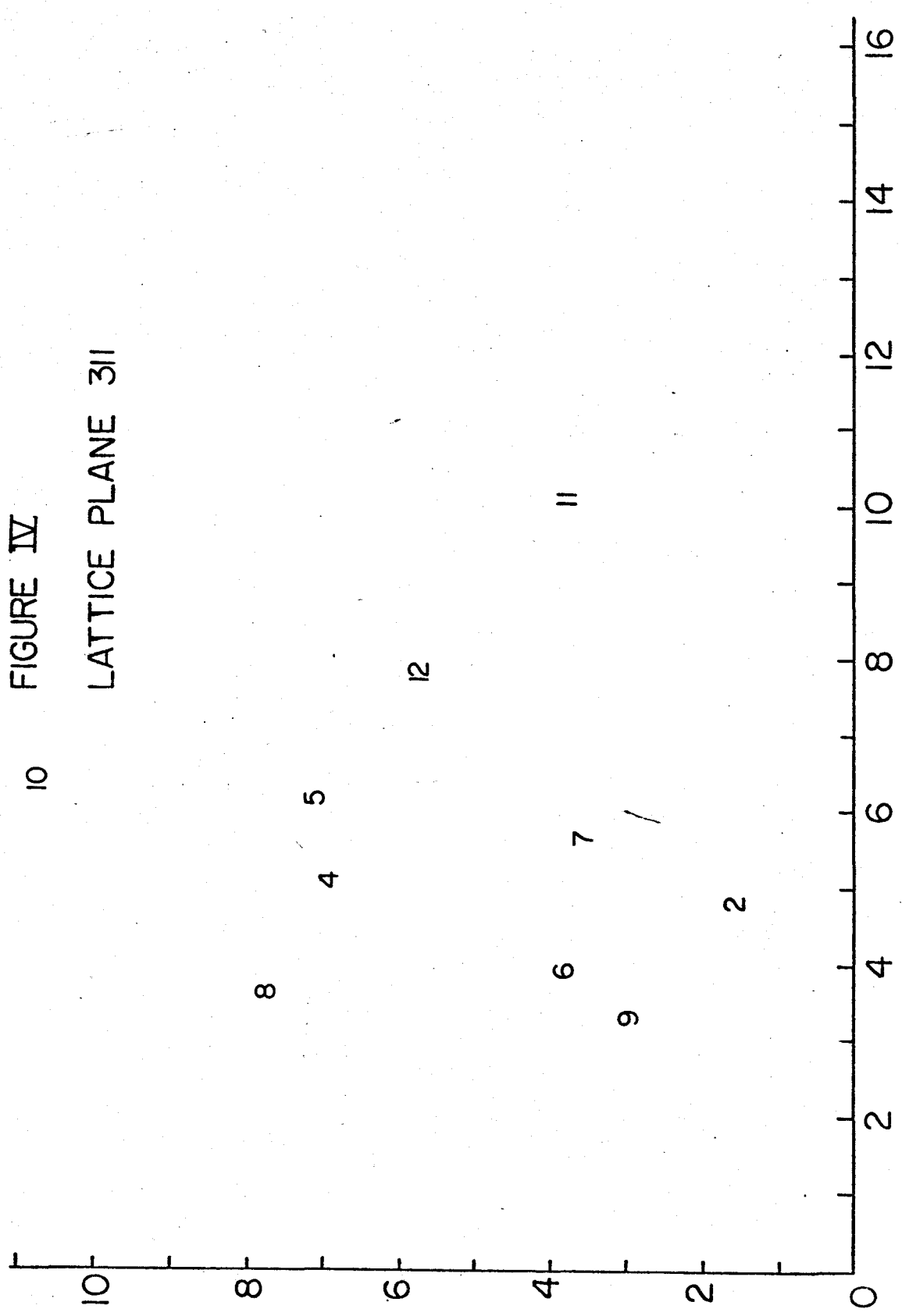


FIGURE IV

LATTICE PLANE 311

CALCULATED ERROR IN Fo. COMPOSITION (WEIGHT %)

MEAN PEAK TO BACKGROUND INTENSITY RATIOS

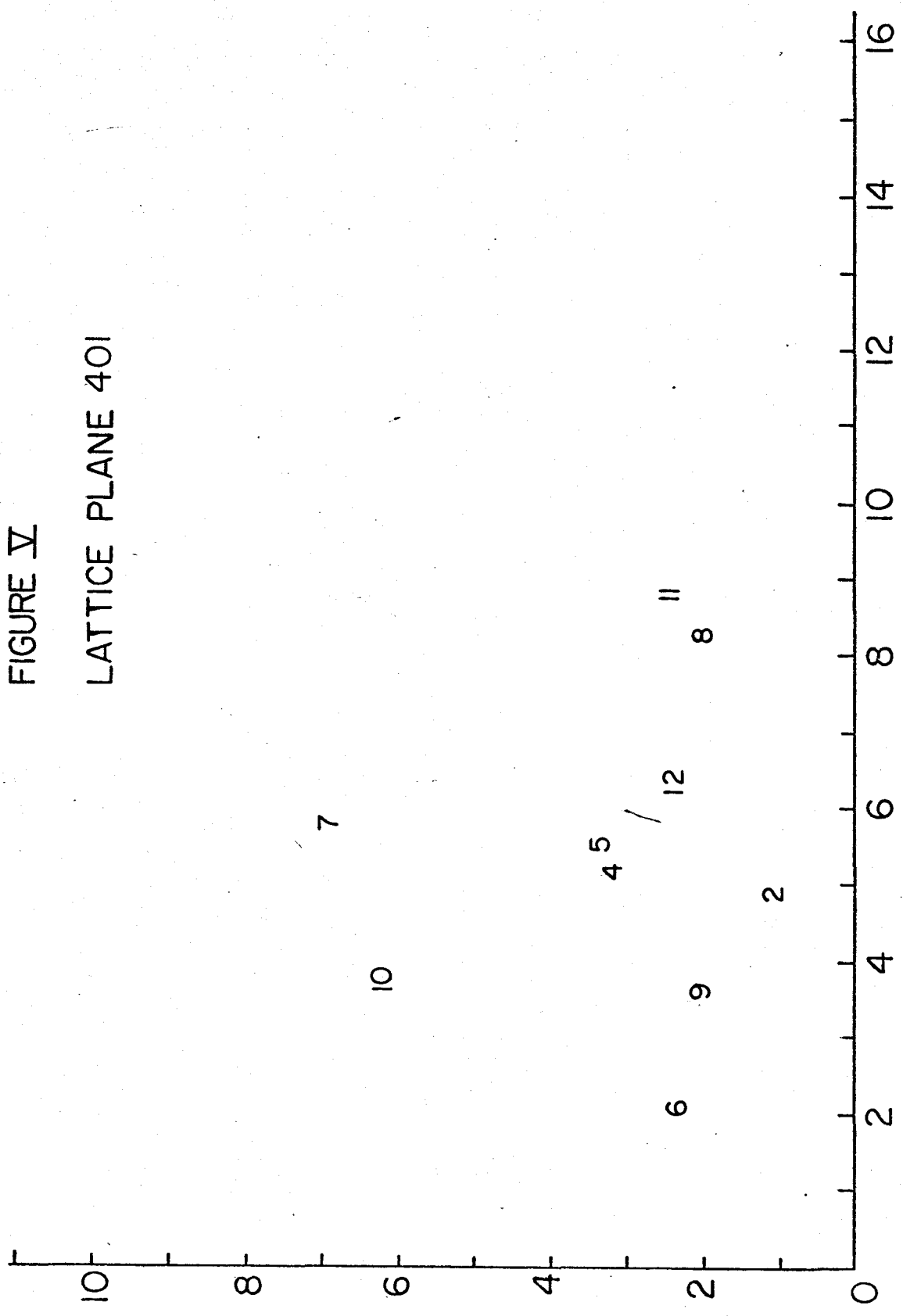


FIGURE V

LATTICE PLANE 401

CALCULATED ERROR IN Fo. COMPOSITION (WEIGHT %)

The lattice plane with the largest peak to background intensity ratio establishes the most reliable overall error in Fo. composition for the experiment. From observation of Figures III, IV and V, olivine sample No. 10 in Figure IV has the greatest peak to background intensity ratio and shows an experimental error for Fo. composition of ± 6.386 wt. % Fo. Thus, the overall experimental error of Fo. determination and reliability of the curves is ± 6 wt. % Fo.

DISCUSSION

(A) Determination of an Olivine of Known Fo. Composition

A sample of known Fo. composition was used to test the reliability of the 3 Fo. determinative curves. Dr. R.H. McNutt donated an olivine, composition 90 wt. % Fo. The known sample was prepared, x-rayed and analysed in an identical manner to each of the Sudbury samples. The resulting Fo. composition as read from the 3 curves in wt. % Fo. was 89, 87 and 85 for (301), (311) and (401) respectively. The reliability of the 3 Fo. determinative curves was ± 6 wt. % Fo. All the calculated Fo. compositions for each plane of the known sample were within the experimental error range.

(B) Effect of Other Elements on the Fo. Determinative Curve

Varying amounts of Ni, Ca and Mn substitute into (Mg, Fe) olivines. The (Mg, Fe) olivine series rarely contain appreciable amounts of Mn and Ca in most natural crystals (Deer et al.). In the Mg rich end of the series small amounts of Ni are usually present (Deer et al.). In order to study the effect of the presence of these 3 elements on the Fo. determination curves, six olivines of varying Mg, Fe, Mn, Ca and Ni composition were used. Table X displays the olivines and their res-

pective lattice parameters. The 2θ and d spacings for each olivine were calculated using equations 1, 2 and 3. Results are also listed in Table X.

Two synthetic olivines, pure forsterite (Mg_2SiO_4) and pure fayalite (Fe_2SiO_4) plus their lattice parameters were obtained from Swanson and Tatge (1951) and Yoder and Sahama (1957) respectively. The 2θ and d spacings were calculated as before. The results are seen in Table XI.

The $\Delta 2\theta$ shift caused by the presence of Ni, Mn and Ca in the Mg_2SiO_4 lattice was observed relative to the "ideal" 2θ for synthetic Fo. From observation of Table X it was noted that Ca and Mn shift the 2θ to a lower angle and Ni to a slightly larger 2θ angle. Similar trends were observed using synthetic fayalite as a reference point for $\Delta 2\theta$ shifts.

The above trending relationship was reversed when d spacing instead of 2θ values were used. This implies a relationship between cation size and $\Delta 2\theta$ shift. Ionic radii of Mg, Fe, Mn, Ca and Ni are listed below:

	rA°	
Ni ⁺²	0.70	↑ increasing 2θ decreasing d decreasing r
Mg ⁺²	0.74	
Fe ⁺²	0.80	
Mn ⁺²	0.91	
Ca ⁺²	1.04	

TABLE X OLIVINES OF VARYING Mg, Fe, Ni, Ca and Mn COMPOSITIONS

	1	2	3	4	5	6
$a(\text{Å})$	10.118	10.577	11.180	11.1466	11.108	11.371
$b(\text{Å})$	5.9105	6.146	6.469	6.4885	6.382	6.782
$c(\text{Å})$	4.7274	4.844	4.892	4.9131	4.822	5.091
$d_{301}(\text{Å})$	2.7456	2.8506	2.9645	2.9635	2.9368	3.0402
$2\theta_{301}^\circ$	32.613	31.380	30.145	30.155	30.437	29.377
$d_{33}(\text{Å})$	2.4900	2.5860	2.6950	2.6957	2.6678	2.7742
$2\theta_{311}^\circ$	36.069	34.688	33.243	33.234	33.591	32.267
$d_{401}(\text{Å})$	2.2303	2.3210	2.4268	2.4239	2.4065	2.4820
$2\theta_{301}^\circ$	40.442	38.798	37.042	37.088	37.367	36.190

- 1 Ni_2SiO_4
- 2 $(\text{Fe}_{.514} \text{Mn}_{.464} \text{Mg}_{.022})_2 \text{SiO}_4$
- 3 $(\text{Ca}_{.568} \text{Fe}_{.432})_2 \text{SiO}_4$
- 4 $(\text{Ca}_{.490} \text{Mn}_{.460} \text{Mg}_{.046} \text{Fe}_{.004})_2 \text{SiO}_4$
- 5 $(\text{Mg}_{.50} \text{Ca}_{.50})_2 \text{SiO}_4$
- 6 $\text{Ca}_2 \text{SiO}_4$

1, 2, 3, 4 are from G. E. Brown Jr. 1970

5 from Onken (1965)

6 from Smith *et al.* (1965)

TABLE XI SYNTHETIC FORSTERITE AND FAYALITE

	FORSTERITE Mg_2SiO_4	FAYALITE Fe_2SiO_4
$d_{301}(\text{A}^\circ)$	2.768	2.829
$2\theta_{301}^\circ$	32.341	31.626
$d_{311}(\text{A}^\circ)$	2.513	2.565
$2\theta_{311}^\circ$	35.728	34.980
$d_{401}(\text{A}^\circ)$	2.250	2.305
$2\theta_{401}^\circ$	40.073	39.077

Mg_2SiO_4 from Swanson and Tatge (1951)

Fe_2SiO_4 from Yoder and Sahama 1957

Observations showed as 2θ of the olivine increases (or d spacing decreases) the abundance of smaller cations (Ni in this study) in the Mg_2SiO_4 lattice increases. Similarly, as the 2θ of the olivines decreases the amount of larger cations (Mn, Ca and Fe) in the Mg_2SiO_4 lattice increases.

The Fo. determinative curve developed and tested in this study was valid for olivines of the (Mg, Fe) isomorphous series only. Natural (Mg, Fe) olivines rarely contain significant amounts of Mn and Ca and Mg-rich olivines include only small amounts of Ni in their structures (Deer et al.). The $\Delta 2\theta$ shift caused by the presence of any one or any combination of the 3 cations in the (Mg, Fe) olivine structure depends on the abundance of these cations in the Fo. structure and, therefore, must be trivial for natural occurring olivines.

CONCLUDING REMARKS AND RECOMMENDATIONS

From the XRD of 10 Sudbury olivines, it was found that the 3 Fo. determinative curves constructed from Birle et al. exhibited a precision of ± 6 wt. % Fo. When the curves were tested with an olivine of known Fo. composition, each curve resolved a Fo. composition within the calculated error of the experimental procedure.

The effect of Ni, Mn and Ca on the Fo. determinative curves was studied. Six olivines of differing Mg, Fe, Ni, Mn and Ca composition from various literature sources were observed. Using the "ideal" 2θ from a synthetic Mg_2SiO_4 (Swanson et al.) as a reference point, it was found that Ni cations in the Fo. olivine structure shifted the 2θ to a larger angle and increasing amounts of Fe, Mn and Ca in the Fo. lattice shifted 2θ to a smaller angle. The situation was reversed when d spacings were used.

The $\Delta 2\theta$ shift caused by increasing amounts of Ni, Ca and Mn was probably trivial as Mn and Ca are rare in natural (Mg, Fe) olivines and small amounts of Ni are found only in Mg-rich olivines (Deer et al.). The substitution of Fe for Mg in the olivine structure caused the greatest $\Delta 2\theta$ shift and this was to a smaller 2θ angle.

Problems encountered in this study were mostly technical. More precision and accuracy could be achieved with a more experienced operator plus new and better analytical methods. To overstep some of the technical problems that existed, different analytical methods could be used to measure Fo. composition either as separate entities or in unison with XRD analysis. XRF, neutron activation and atomic absorption could be reasonable alternatives to XRD.

XRF involves similar experimental problems as XRD analysis. They are absorption and enhancement by the sample, inhomogeneities in the sample and instrumental instabilities (personal communication with Dr. H. D. Grundy 1972). A greater volume and more purity of the sample would be required.

Neutron activation could also be used. Isotope ${}_{12}^{28}\text{Mg}$ has a half life of 21 hours (Handbook of Chemistry and Physics) which is sufficiently long enough to enable neutron activation analysis of Fo. composition. The ever presence of Fe in natural (Mg, Fe) olivines would pose an analytical problem (personal communication with W. P. Binney 1973).

Atomic absorption yields a more quantitative analysis than XRD. The sample being analysed has to be of greater purity than with XRD analysis because this technique cannot distinguish between the presence of Mg in Fo. or the contaminants present. To overcome the problem of purity,

the olivines would be separated magnetically as before but further purification steps must be taken. The olivine samples could be subjected to differential settling in density layered liquids and then preferentially dissolved using weak acids that would dissolve only olivines and not attack existing contaminants (personal communication with P. D. Rice and A. G. Sherin 1973).

It would seem that a combination of analytical methods would provide a more reliable estimate of the Fo. composition of olivines.

REFERENCES

- Adler, I. (1966) X-ray Emission Spectrography in Geology; Elsevier Publishing Co., Amsterdam.
- Azaroff, Leonid V. and Buerger, Martin J. (1958) The Powder Method. New York: McGraw-Hill Book Co.
- Birle, J.D., Gibbs, G.V., Moore, P.B. and Smith, J.F. (1968) Crystal structures of natural olivines; American Mineralogist 53, 807-824.
- Brown, G.E. (1970) Crystal Chemistry of the Olivine. Virginia Polytechnic Institute, Ph.D., Mineralogy.
- Chemical Rubber Co., The (1969-1970) Handbook of Chemistry and Physics, College Edition, 50th Edition.
- Deer, W.A., Howie, R.A. and Zussman, J. (1962) Rock Forming Minerals: Volume 1 Ortho- and Ring Silicates. Longmans, Green and Co. Ltd., London.
- Onken, H. (1964) Vereinigung der Kristallostruktur von Monticellite. Naturwissenschaften, 51, 334.
- Smith, D.K., Majumdar, A. and Ordway, F. (1965) The crystal structure of γ -dicalcium silicate. Acta Crystallog., 18, 787-795.

Swanson, H. E. and Tatge, E. (1951) J. Res. NBS, 46, 325.

Yoder, H. S. and Sahama, Th. G. (1957) Olivine X-ray determinative
curve. American Mineralogist, 42, 475.